ORIGINAL ARTICLE

Multi-roll levelling for wave defects of metal sheets based on the beam-membrane method

Guodong Yi [1] · Yang Wang [1] · Xiaojian Liu [1,2] · Chao Wang [1]

Abstract

Wave defects are the main flatness defects in rolled metal sheets and typically must be eliminated via multi-roll levelling for further use. Convex work rolls are the key component of the levelling process. The effectiveness of the description of the work roll and its bending characteristics determines the efficiency and accuracy of the levelling numerical analysis, which is also the key problem to be solved in the current research. This paper proposes a finite element expression method for convex work rolls that is based on the beam-membrane method by using a beam element to express the mechanical characteristics of the work rolls and the membrane elements to express the contact characteristics between the work rolls and the metal sheet. An effective multi-roll wave levelling model was established based on the beam-membrane method, and the influence of the bending parameters of the work rolls on the wave levelling performance was analysed. The results demonstrate that work rolls that have a parabolic bending curve can substantially reduce, but not eliminate, residual waves. The residual stress and curvature simulation have been discussed, and the comparison shows that the proposed method is closer to the real experiment result.

Keywords Roll levelling · Metal sheet · Wave defects · Beam-membrane method · Bending parameters

1 Introduction

Metal sheets are widely used in the manufacturing industry and are mainly produced via cold rolling or hot rolling. Typically, a variety of flatness defects are present in a rolled metal sheet, including waves, bends, and other defects that are caused by residual stress. Waves are the main flatness defects and include middle waves and side waves [1–3]. The origin of wave defects during rolling is thermo-elastic deformation of the roll and the heterogeneity of the stress field results in heterogeneous plastic deformation [2–4]. During the rolling forming of the steel sheet, the steel sheet is deformed and extended in one direction, and the rolled steel sheet has a certain directionality, which is said to be longitudinal along the rolling direction, that is, the fibre direction of the sheet. The fibre here refers to the crushed and elongated crystal grain

structures in the rolling process. The longitudinal fibre length of the sheet is unevenly distributed along the width direction, thereby causing longitudinal internal stress in the sheet, which results in wave formation when the internal stress exceeds the ultimate stress of the sheet. If the fibres at the edge of the sheet are longer than the fibres in the middle, edge-waves are formed, whereas if the fibres in the middle of the sheet are longer than the fibres at the edge, middle-waves are formed [2, 5–7]. It is necessary to reduce or eliminate the wave defects before the sheet is used.

As an important process for improving the flatness of the sheet, multi-roll levelling eliminates wave defects by applying a progressively elastoplastic bending deformation to the sheet [8, 9]. Under the radial load that is applied by the back-up rolls, the work rolls are bent to a specified convexity and a gap of varying width is formed between the work rolls; hence, the longitudinal elongations of the processed sheets differ in the width direction [10, 11]. By precisely controlling the gap width according to the type and size of the wave defects, the length of the longitudinal fibre of the sheet can be made uniform, thereby improving the flatness of the sheet [12].

An analytical method and a finite element method are the two main methods that are used in the levelling analysis of metal sheets.

✉ Xiaojian Liu
liuxj@zju.edu.cn

1 School of Mechanical Engineering, Zhejiang University, Hangzhou 310027, China

2 Ningbo Research Institute, Zhejiang University, Ningbo 315100, China

In the analytical method, the work roll and the metal sheet are typically modelled as beams for analysis and solution. Doege et al. [8] presented an analytic formation model that analyses the levelling process of one-dimensionally curved sheet metal. Chen et al. [10] proposed a 2.5-dimensional analytical approach to investigate the essential deformation law of levelling for plates with transverse waves, in which the plate was transversely divided into some strips with equal width, and the bending deformation of each strip and the leveling effect of overall plate were obtained by comprehensive consideration of various strips along with the width. Baumgart et al. [13] presented a physics-based mathematical model, in which the work rolls of the leveller are modelled as Euler–Bernoulli beams, and the load distribution was derived by dividing the plate into narrow parallel beams and modelling the force-deflection relation individually for each beam. Liu et al. [14] developed an analytical model for predicting the H-beams levelling process with the computational procedure of describing the continuous bending and reversed bending process, as well as the unloading process. Brauneis et al. [15] presented a mathematical deflection model of a leveller for cold heavy plates, in which the work rolls were modelled as Euler–Bernoulli beams to solve the static beam equation with multiple complex boundary conditions, and the plate was divided into several independent stripes and modelled as beams to simplify the calculation of the distributed forces exerted on the work rolls due to the levelling deformation of the plate. Brauneis et al. [16] presented a fast and robust mathematical levelling model to iteratively solve the static beam equation of an elastoplastically deformed Euler–Bernoulli beam during the levelling process of steel plates. Yu et al. [17] analysed the deformation path in the roller gap, and the graphic method and mathematical induction are adopted to analyse the deformation process of the section of the bar, and proved that although the initial curvature of each section of the bar is different, the difference of initial curvature is eliminated by the reciprocating bending, and the process mechanism of the two-roller straightening is revealed.

In the finite element method, typically, the work roll is defined as a rigid body [11, 18–23] or a rigid surface [24, 25] due to the negligible deformation in forming or levelling, and the metal sheet is discretised as a deformable continuum body [11, 23] and modelled using various types of elements, such as the 4-node shell element [11, 18, 22, 24] and the 8-node hexahedral element [20, 21, 25, 26]. To reduce the computational costs, Woo and Grüber et al. [22, 23] defined a sub-model in which

a fine mesh was used in the greater deformation zone and a coarser mesh was used in the web zone of the sheet. Traub et al. [27] designed a global model and a sub-model for levelling: the global model guarantees a consideration of all boundary conditions applied by the roll forming process, and the sub-model offers the required high resolution of the strain distribution in the bending zone.

Comparative analysis results demonstrate that the analytical method far outperforms the finite element method in terms of computational efficiency with the same level of accuracy; however, the latter is more effective in the analysis of complex structures [9, 14, 16, 28, 29].

In view of these results, various compromise methods have been proposed. Nakhoul et al. [3] addressed the problem of flatness defects using a completely coupled model that combines the FEM for strip elastic-viscoplastic deformation, a powerful semi-analytical model of roll elastic deformation, and a simple model of buckling that is based on an elastic/buckling deformation decomposition. Nakhoul et al. [4] presented a simple buckling model that can be coupled to a finite element rolling model and applied to practical questions concerning flatness in cold strip rolling. Dratz and Silvestre et al. [9, 28] presented a semi-analytical model based on a discrete bending theory, which was a good compromise between precision and speed calculation. Su et al. [30] proposed a method of quantifying the projection track regarding the edge of the profile section in the horizontal plane that follows a cubic curve and uses the curve function to reasonably distribute the bending angle to study the maximum forming strain and the average strain for all passes of the sheet between the forming passes. Lee et al. [31] proposed a combination of the finite element analysis and the analytic model based on curvature integration method to investigate the moment-curvature relationship of the metal sheet and the proper positions of the rolls corresponding to the optimal curvature, respectively. Weiss et al. [32] formed an aluminium foam sandwich material by V-die bending and roll forming, and observed that the higher material formability in roll forming compared with that in V-die bending was attributed to a more evenly distributed contact pressure and more homogeneous forming, combined with a continuous contact of the metal sheet with the top and bottom rolls. Abdelkhalek et al. [2, 33, 34] presented a coupled approach for flatness defect prediction in thin plate rolling, in which a simple buckling criterion was introduced in the FEM model of strip and roll deformation; hence, the stresses were closer to experiments.

In the finite element method for levelling analysis that is discussed above, the description of the work roll affects the accuracy and speed of the calculation. Therefore, this study proposed a finite element expression method for convex work rolls that is based on the beam-membrane method (BMM), which uses a beam element to express the mechanical characteristics of the work rolls, and membrane elements, which are used to express the contact characteristics between the work rolls and the metal sheet. An effective multi-roll wave levelling model was established based on the beam-membrane method and the influences of the bending parameters of the work rolls on the wave levelling effect were analysed.

2 Expression of the work roll based on the BMM

During the levelling process, the straight work roll is bent and becomes convex due to the radial force that is applied by the back-up rolls. Therefore, the work roll must be modelled as a flexible body instead of a rigid body in the finite element model. Simulations have shown that the transformation from a rigid body to a flexible body with 3D solid elements is a time-consuming calculation and usually ends in failure in our experiments.

In the multi-roll levelling process, the work rolls and the sheet are elastically deformed and elastoplastically deformed, respectively, and there is a line contact between them. The levelling is mainly affected by the bending condition of the work roll, regardless of its internal condition. According to this feature, a finite element model of the work roll that is based on the BMM is proposed.

The BMM uses a multi-point constrained combination of a beam element and membrane elements to express a convex work roll. The bending of the work roll is an elastic deformation, which can be accurately expressed by using a beam element of a circular cross-section with a minimum number of nodes. However, the beam element does not support contact with other elements and cannot solve the nonlinear multi-body contact problem in the multi-roll levelling. Therefore, membrane elements are used to express the outer surface of the work roll and its contact characteristics with the metal sheet. Another alternative is a shell element; however, it has six degrees of freedom and contains multiple layers, while a membrane element has only three degrees of freedom of movement and is single-layered, which can substantially reduce the computation time and has no adverse effect on the model.

The construction of the finite element model of the convex work roll that is based on the BMM is illustrated in Fig. 1. The mechanical characteristics, such as stiffness, strength, and convexity, of the work roll are expressed by a beam element that is located at its axis and the outer surface of the work roll and its contact
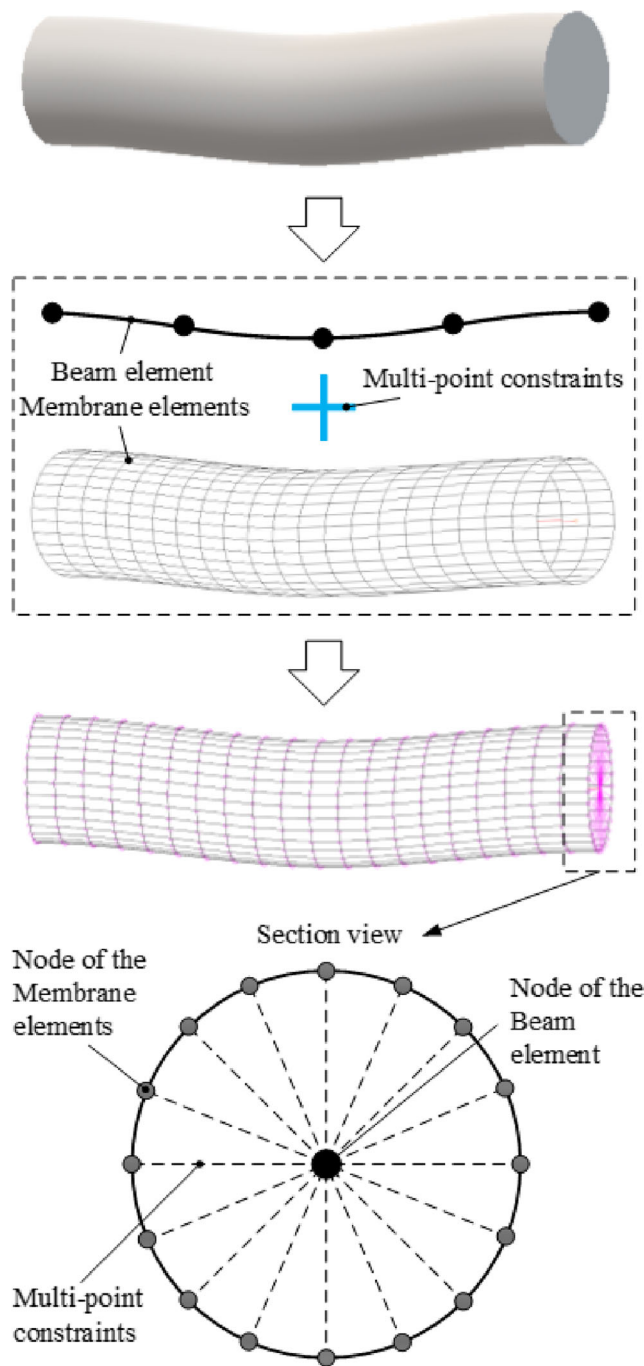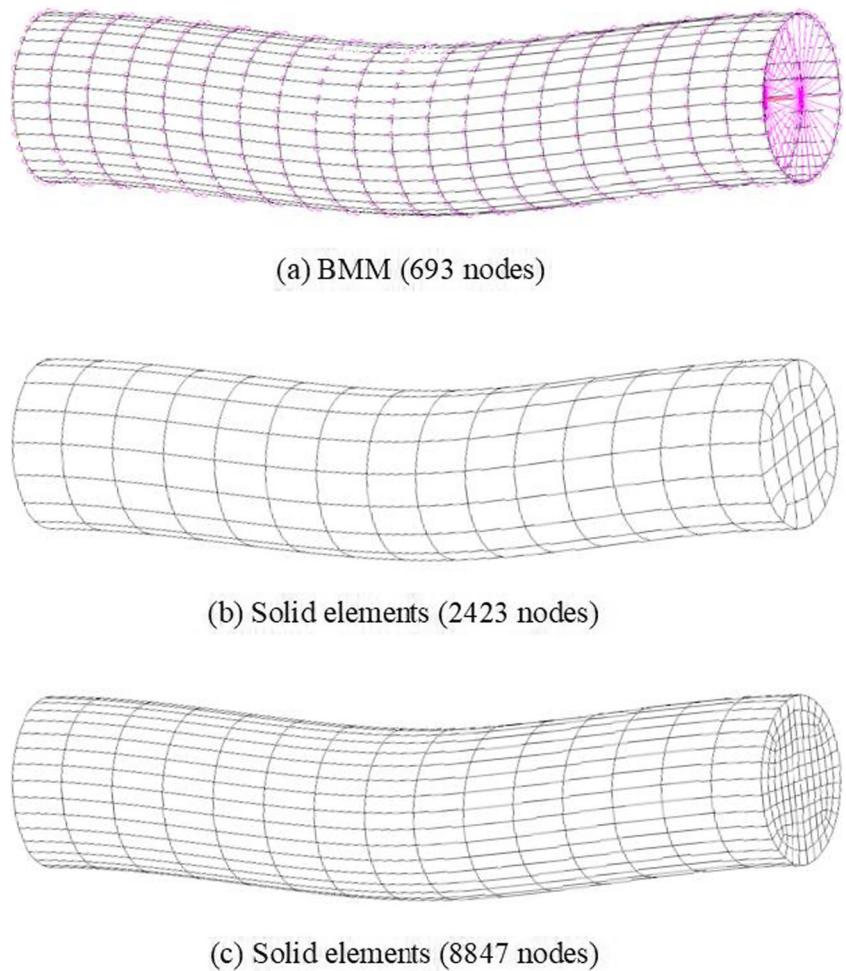

Fig. 1 Finite element model of the convex work roll that is based on the BMM

Fig. 2 Work rolls that are expressed with the BMM and solid elements

(a) BMM (693 nodes)

(b) Solid elements (2423 nodes)

(c) Solid elements (8847 nodes)

characteristics with the metal sheet are expressed by the membrane elements. In a cross-section of the work roll, all the degrees of freedom of one node of the beam element and all nodes of the membrane elements on the circumference are bound by multi-point constraints; hence, the bending characteristics that are expressed by the beam element can be transmitted to the membrane elements and act on the metal sheet.
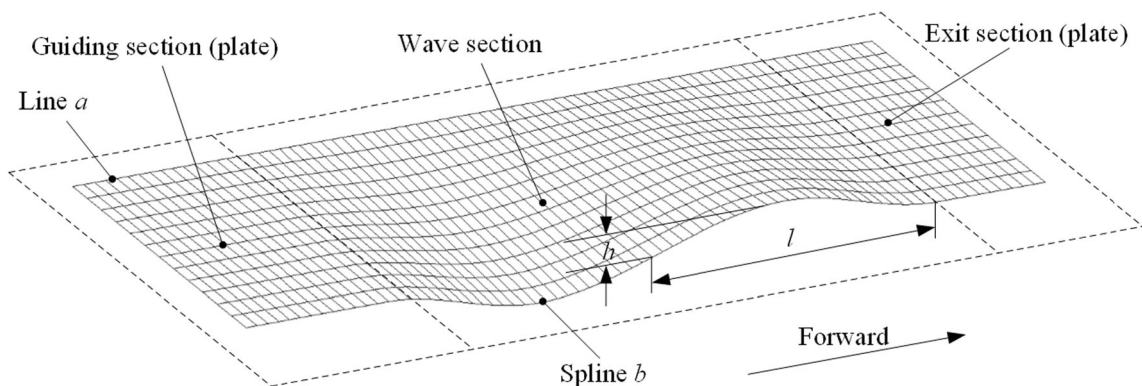

Fig. 3 Finite element model of a metal sheet with wave defects

The following is a comparative analysis of the work rolls that are expressed by the BMM and by the 3D solid elements. A 20-node regular hexahedral element that has satisfactory bending characteristics is selected as the 3D solid element. Figure 2 shows three expression schemes for the work rolls. Scheme (a) is expressed with the BMM and has 32 equally spaced nodes in the circumferential direction, for a total of 693 nodes. Scheme (b) is expressed with solid elements and has 16 equally spaced nodes in the circumferential direction, for a total of 2423 nodes. Scheme (c) is also expressed with solid elements and has 32 equally spaced nodes in the circumferential direction, for a total of 8847 nodes. The larger the number of nodes in the circumferential direction, the higher the contact accuracy.

When the total number of nodes exceeds 1000, the calculation time of the model is proportional to the square of the number of nodes. Among the three schemes that are shown in Fig. 2, the total number of nodes with the BMM is 28.6% and 7.83% of those of the latter two schemes, respectively, and the calculation time of the BMM is 8.2% and 0.61% of those of the latter two schemes. Therefore, the BMM can substantially reduce the calculation time, which enables the practical application of the numerical simulation of multi-roll levelling for wave defects. In addition, simulation experiments show that the solution of the simulation model that uses the 3D solid elements to express the work roll usually fails or yields severely distorted results.

# 3 Finite element expression of a metal sheet with wave defects

There are two problems in the finite element expression of a metal sheet with wave defects: expressing the flexibility of the sheet and expressing the wave defects.

Solid elements, which are widely used in the numerical simulation of medium and heavy sheets, are not suitable for thin sheets because the thickness of thin sheets is substantially smaller than the length and width. When the thickness of the model is reduced by half and the other dimensions are unchanged, the number of elements in the model is four times that of the original model while keeping the ratio of the length, width, and height of each unit constant.

The number of elements will be reduced if the width and length of the elements are increased; however, it will make the unit slim and reduce the calculation accuracy. The ratio of the longest to the shortest dimension of the hexahedral element must not exceed 10; otherwise, the calculation results will be distorted. For a thin sheet, if the length, width, and height of the

element are kept constant, the number of elements is inversely proportional to the square of the thickness, which renders the numerical simulation of multi-roll levelling, which is easy to implement for medium and heavy sheets, infeasible for thin sheets.

In this study, shell elements with thickness properties are used to express the sheet; hence, the total number of elements
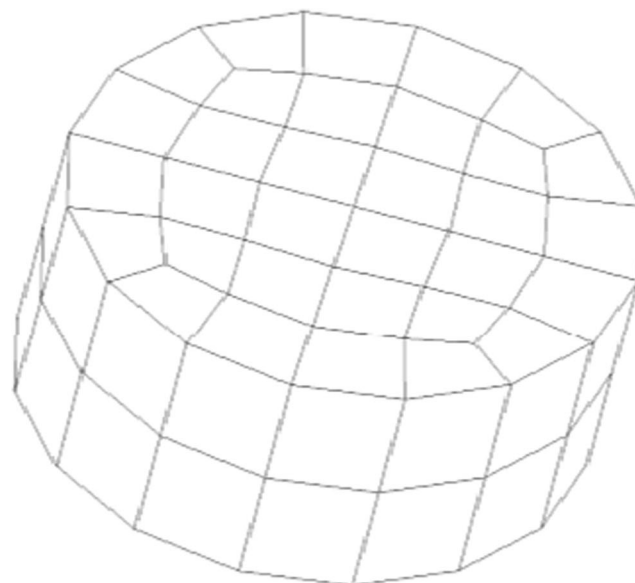
(a) Discrete elements
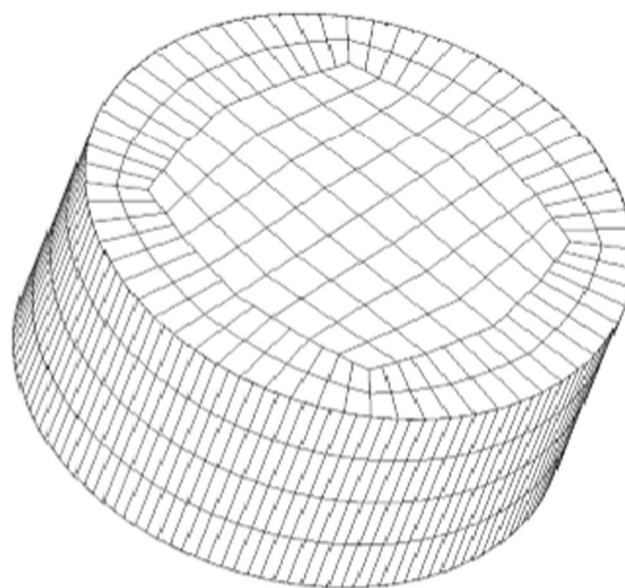
(b) Coons surface

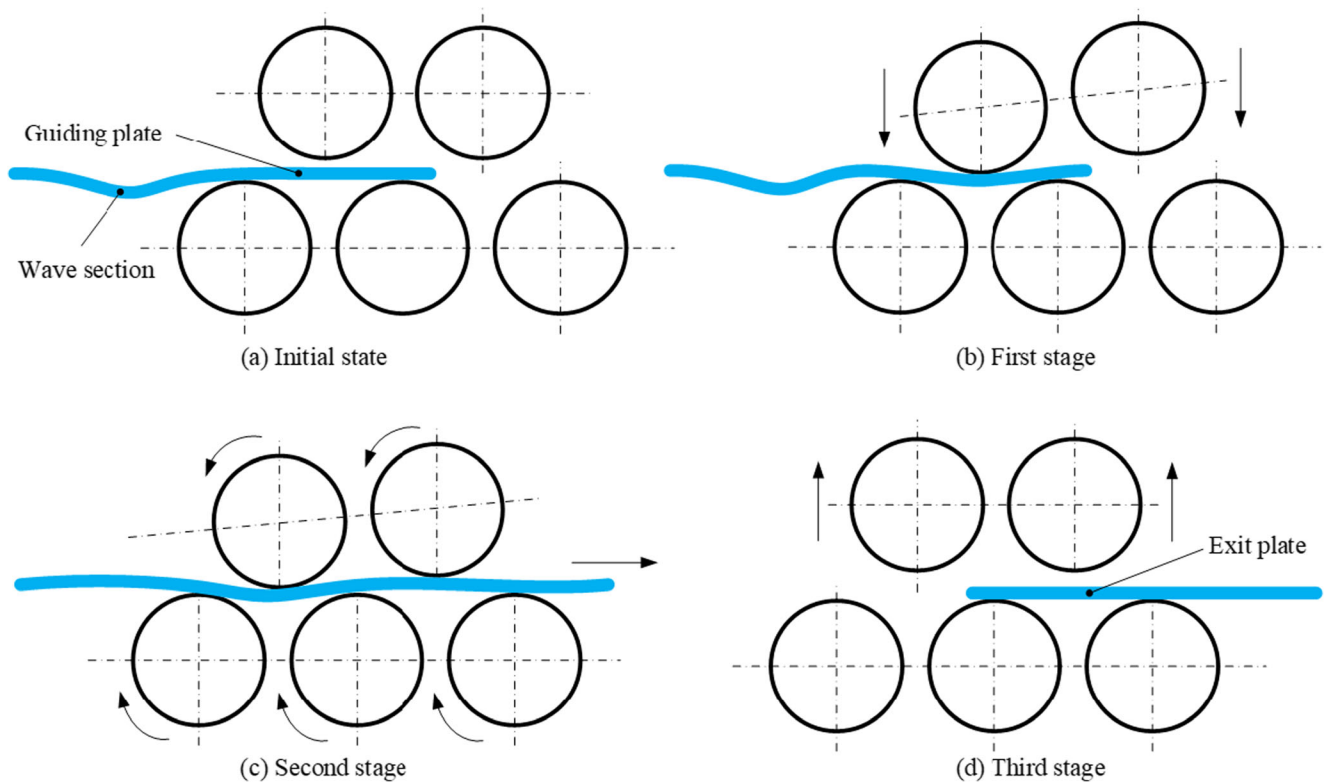Fig. 4 Representations of the outer surface of the work roll

Fig. 5 Process of multi-roll wave levelling

that are obtained via meshing is unaffected by the thickness. The shell element has superior bending properties compared with the solid element due to the six degrees of freedom of each node and is more suitable for the repeated alternating bending processes of multi-roll levelling.

The wave defect of the sheet is expressed in terms of the height h and the length l of the wave, as illustrated in Fig. 3. The finite element model of a sheet with wave defects is constructed as follows: First, a line a and a multi-segment cubic spline b are established such that b passes through the key point that expresses the height and length of the wave. Second, the straight line a and the spline b are staked to generate a curved surface. Third, the surface is meshed with shell elements to generate a finite element model of the sheet.

As illustrated in Fig. 3, the finite element model of the sheet is divided into three parts: the guiding section, the exit section, and the wave section, which needs to be levelled.

4 Multi-roll levelling model for wave defects

After the effective expression of the work roll and the metal sheet, there remain two key issues to be overcome in establishing the multi-roll levelling model for wave defects, namely the modelling of the contact between the work rolls and the sheet and the definition of the wave levelling process, which determine the accuracy and efficiency of the calculation.

4.1 Modelling of the contact between the work rolls and the sheet based on Coons surfaces

In the multi-roll wave levelling model, the sheet is defined as a flexible body and the lower work rolls must

Table 1 Multi-roll levelling parameters

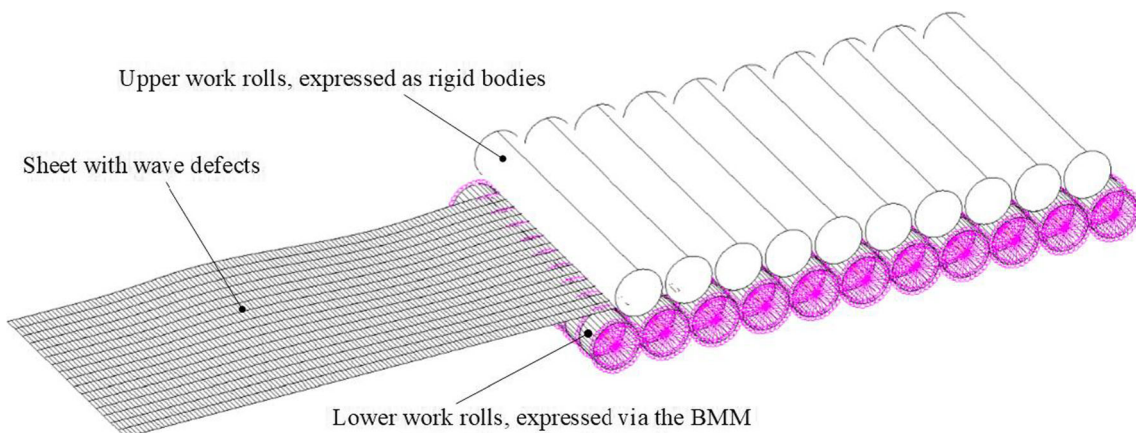| Parameter	Value
Number of work rolls	21
Diameter of work rolls (mm)	47
Distance between work rolls (mm)	50
Yield stress (MPa)	400
Modulus of elasticity (GPa)	200
Poisson's ratio	0.28
Thickness of the sheet (mm)	1.0
Width of the sheet (mm)	1000
Sheet element type	SHELL93

Fig. 6 Finite element model that is based on the BMM for multi-roll wave levelling

be defined as flexible bodies because of the sheet's bending characteristics, whereas the upper work rolls can be defined as rigid bodies to save calculation time.

In the levelling process, the work rolls are in line contact with the sheet; hence, the roundness precision of the work roll must be high. However, in the finite element model, the surface of the work roll is composed of discrete elements, that is, the circle is represented by a regular polygon. The accuracy increases when the number of sides of the polygon is increased; however, the number of elements and the calculation time also increase substantially.

High-precision contact can be achieved with fewer elements if Coons surfaces are used instead of discrete elements to express the outer surface of the work rolls. The circularity accuracy of the outer surface of the

work roll is low in Fig. 4a (expressed by 16 discrete elements) and high in Fig. 4b (expressed by a Coons surface instead of discrete elements) and the calculation time of the latter does not exceed that of the former.

Contact calculations are highly time consuming due to their nonlinear iteration. In the multi-roll levelling process, only the work rolls are in contact with the sheet and not every flexible body is in contact with all other flexible and rigid bodies. For example, there are 21 actual contact pairs in the 21-roll levelling model; however, in the worst case, due to poor settings, it will contain 264 contact pairs and the calculation time will be 10 times longer compared with that of the former.

In multi-roll levelling, the upper and lower surfaces of the shell elements on the sheet are in contact with

Fig. 7 Roll curve for levelling wave defects
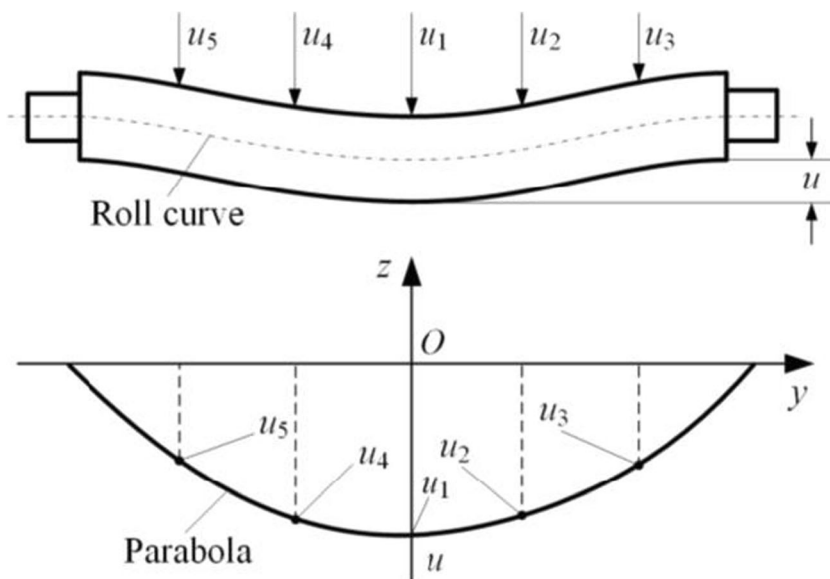
the upper and lower work rolls, respectively. Only the outer surfaces of the membrane elements on the work rolls are in contact with the sheet; the inner surface is not in contact with any other elements. These factors reduce the number of contact calculations by nearly half and the computation time is reduced substantially.

4.2 Analysis of the wave levelling process

The initial state of the sheet in the levelling simulation determines whether it can be fed correctly into the leveller, which has a serious impact on the calculation efficiency and accuracy.

There are two methods for initial state definition of the sheet: The first is the addition of a guiding wedge at the front end of the sheet, with two bevels tangential to the upper and lower work rolls. The sheet is correctly fed by the friction after the work roll rotates. The other is the addition of a guiding plate at the front end of the sheet, which traverses the gap among all the work rolls. The sheet is successfully fed after the upper work rolls move down. The main advantage of the first method is that the number of elements that are used by the guiding wedge is small; hence, the simulation time is not substantially increased. However, the feeding effect is unsatisfactory due to the staggered centres of the upper and lower work rolls. The feeding effect of the second method is satisfactory; however, the guiding plate uses many elements, which leads to a substantial increase in the calculation time.

On the basis of the second method, in this study, the guiding plate only passes through the gaps of the first three work rolls instead of all the work rolls, as shown in Fig. 5a. The work rolls that have been in contact with the sheet push the sheet forward under friction to come into contact with the subsequent work rolls. The simulation experiment demonstrates that compared with the second method, the guiding plate in this method is substantially shortened and the reduction of the number of elements decreases the calculation time of the model.

Multi-roll wave levelling is a quasi-static process that has three stages: first, the upper work rolls are moved down and the lower work rolls are bent; second, all the work rolls rotate to start the levelling process; and third, the upper work rolls are moved up and the sheet rebounds to a free state.

In the first stage, all work rolls are at rest and the bending parameters are set. As illustrated in Fig. 5b, the upper work rolls are arranged at a specified inclination angle and the lower work rolls are bent into a specified convexity.

The second stage is the main part of the levelling process, in which all the work rolls rotate at a constant speed and process the sheet as illustrated in Fig. 5c.

The elastoplastic bending deformation of the sheet is gradually reduced between the work rolls to a nearly flat state at the exit.

In the third stage, the upper work rolls are moved up and the radial loads of the lower work rolls are removed, thereby leaving the sheet in a free state, as shown in Fig. 5d. However, in the completely free state, the sheet is prone to instability during the simulation. The solution is to add an exit plate at the end of the sheet, as illustrated in Fig. 3. After the wave section of the sheet has completely exited the gap among the work rolls, the exit plate remains between the last three work rolls to ensure that the sheet is pressed and will not destabilise. At this time, bending of the exit plate may occur, which would result in a rigid displacement of the wave segment; post-processing calculations must be performed to eliminate this rigid displacement.

5 Simulation and discussion of the multi-roll levelling

5.1 Finite element model of multi-roll levelling based on the BMM

To simulate the multi-roll levelling process and analyse the influence of bending parameters, the multi-roll levelling model for finite element analysis based on the BMM has to be built. The model was developed by Patran Command Language (PCL), on the platform of MSC. Patran as the pre-processor and MSC.Marc as the solution. The simulation was implemented on a computer with 4.0-GHz CPU and 16GB RAM. Beam element and membrane element are connected by multi-point constraints in Patran, and are used as a whole to express the work roll with convexity. In a cross-section of the work roll, the BMM bounds all the degrees of freedom of one node of the beam element and all nodes of the membrane elements on the circumference, using the multi-point constraints of RBE2. Hence, the bending characteristics that are expressed by the beam element can be transmitted to the membrane elements and act on the metal sheet.

The biggest difficulty with the modeling process is to create the multi-point constraints of RBE2. It requires the determination of two fundamental factors: independent nodes and non-independent nodes, respectively, corresponding to beam element nodes and membrane element nodes that express work rolls.

The detailed PCL procedure that determines the multi-point constraints is summarised in Algorithm 1.

Algorithm 1 Determination of the multi-point constraints in PCL

---

1 Variable definitions
STRING uil_list_create_current_list[VIRTUAL]
GLOBAL STRING lista[VIRTUAL]
string select_rbe_nodes[500](2)
real coord_val(6)

2 Multi-point constraints creation of work roll by double looping
for(i=1 to n2 by 1)
    for(j = 0 to mesh_n3 by 1)

3 Non-independent nodes storage into listb
      coord_val(1) = p*(i-1)-roll_r-0.5
      coord_val(2) = -0.5*s-roll_r
      coord_val(3) = L_down/mesh_n3*j
      coord_val(4) = p*(i-1)+roll_r+0.5
      coord_val(5) = 0.
      coord_val(6) = 0.
      uil_list_b.clear(   )
      list_create_node_att_value(coord_val,
[TRUE, FALSE,   @
      TRUE], ["range", "equal", "equal"], [0.05,
0.05, 0.5], "Coord 0" @
      , "listb", uil_list_create_current_list)

4 Potential sheet nodes removal from listb
      uil_list_a.clear(   )
      list_create_node_ass_group(["roll_fem"], 1,
"lista",   @
      uil_list_create_current_list)
      uil_list_boolean.create("and")
      uil_list_b.replace(   )

5 Independent nodes storage into listb
      coord_val(1) = p*(i-1)
      coord_val(2) = -0.5*s-roll_r
      coord_val(3) = L_down/mesh_n3*j
      coord_val(4) = 0.
      coord_val(5) = 0.
      coord_val(6) = 0.
      uil_list_a.clear(   )
      list_create_node_att_value(coord_val,
[TRUE, TRUE, TRUE], ["equal", @
      "equal", "equal"], [0.05, 0.05, 0.5], "Coord
0", "lista", @
      uil_list_create_current_list)

6 Independent nodes removal from listb
      uil_list_boolean.create("b-a")
      uil_list_b.replace(   )

7 Multi-point constraints creation of RBE2
      select_rbe_nodes(1) = listb
      select_rbe_nodes(2) = lista
      fem_create_mpc_nodal2((i-1)*(mesh_n3+1)
+j+1, "RBE2", 0., 2, [TRUE, @
      FALSE], ["0", "0"], select_rbe_nodes,
["UX,UY,UZ,RX,RY,RZ", ""])
    end

Metal sheet is defined by SHELL93 element in the BMM during the simulation. SHELL93 is particularly well suited to model curved shells. It has six degrees of freedom at each node: translations in the nodal x, y, and z directions and rotations about the nodal x, y, and z axes. SHELL93 element has plasticity, stress stiffening, large deflection, and large strain capabilities. Thickness of the sheet is set as an attribute of the shell element; in this way, the total number of metal sheet elements will not be affected by the sheet thickness. This could significantly reduce the computation of metal sheet simulation. The SHELL93 element has better bending characteristics than solid elements, and is more suitable for the repetitive alternating bending process of multi-roll levelling.

Metal sheets that require multi-roll levelling have good plasticity, so they are modelled using ideal elastoplastic materials, regardless of the strengthening of the material. This is suitable for common low-carbon steels. Q420 steel is a Chinese steel grade of low-alloy high-strength structural steel. It has high strength, especially in normalised or normalised plus tempered state, with high comprehensive mechanical properties, and can be used in large ships, bridges, power station equipment, medium- and high-pressure boilers, high-pressure vessels, lifting machinery, mining machinery, and other large welded structural parts. The material properties we modelled are as follows: yield strength is 400 MPa, modulus of elasticity is 200 GPa, Poisson's ratio is 0.280, and the material density is 7.85 g/cm^3.

According to the parameters that are listed in Table 1, the finite element model based on the BMM for multi-roll wave levelling is established, as illustrated in Fig. 6.

In Fig. 6, the lower work rolls with curvature are expressed via the BMM, the upper work rolls are expressed as rigid bodies, and the sheet is expressed as elastomer using the SHELL93 elements, wherein the height and length of the waves are 10 mm and 200 mm, respectively.

The bending parameters of the work rolls in the model are adjusted using five back-up rolls, which are denoted as u_5, u_4, u_1, u_2, and u_3 from left to right, and the maximum value, which is denoted as u, is equal to u_1. The setting of the five bending parameters requires necessary simplifications because the dynamic adjustment based on the detection results of the sheet defects is highly complicated. As illustrated in Fig. 7, the bending parameters, namely u_1, u_2, u_3, u_4, and u_5, are calculated using the maximum u and a curve equation $z = f(y)$, which is a basic parabolic equation in this study.

The model that needs to be solved is a highly nonlinear problem. In the initial condition, the sheet is tangent to the first and second rolls; all rollers have an angular velocity of 127 rad/s. By virtue of the rotation of the rollers, the sheet is driven forward and thus produces a plastic deformation of the inverse curvature to counteract the initial curvature. The materials of work rolls and metal sheet are low-carbon structural steel. The contact type between the rolls and the sheet is fractional contact,
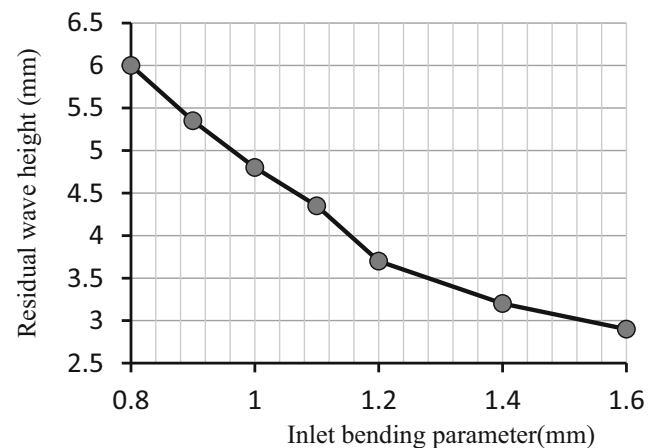

Fig. 8 Effect of the inlet bending parameter on the residual wave height

with the static friction factor of 0.18, regardless of the influence of gravity. In the contact setting, target bodies are the rolls, contact body is the sheet, and contact behaviour is asymmetric. Fixed constraints are applied on the rollers. The force acting on the sheet is periodic strain force with the cycle T of 0.0008 s, which can be simplified to the alternating stress of the T cycle. Alternating stress of 20 MPa on the sheet is applied during the simulation, performing the alternating stress test 12 times. The solution algorithm is penalty function method.

6 Influence of the bending parameters on the wave levelling

Figure 8 depicts the relationship between the inlet bending parameter and the wave levelling results, with a wave height of 10 mm prior to levelling. When the inlet bending parameter increases from 0.8 to 1.2 mm, the residual wave height decreases significantly after levelling, but as the inlet bending parameter continues to increase, the residual wave height decreases slowly.

Figure 9 depicts the relationship between the bending value and the wave levelling results, while the inlet bending
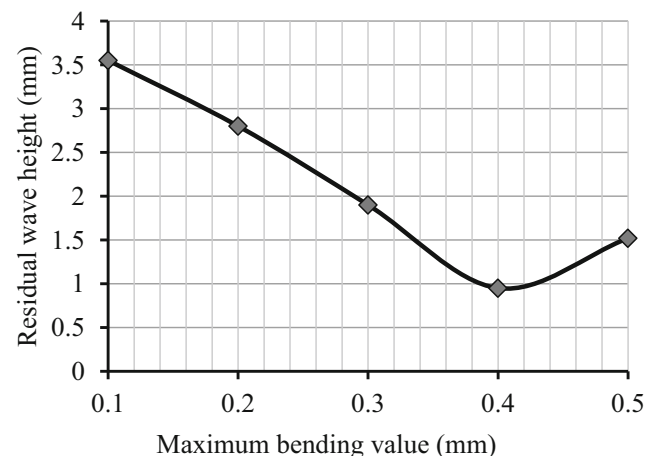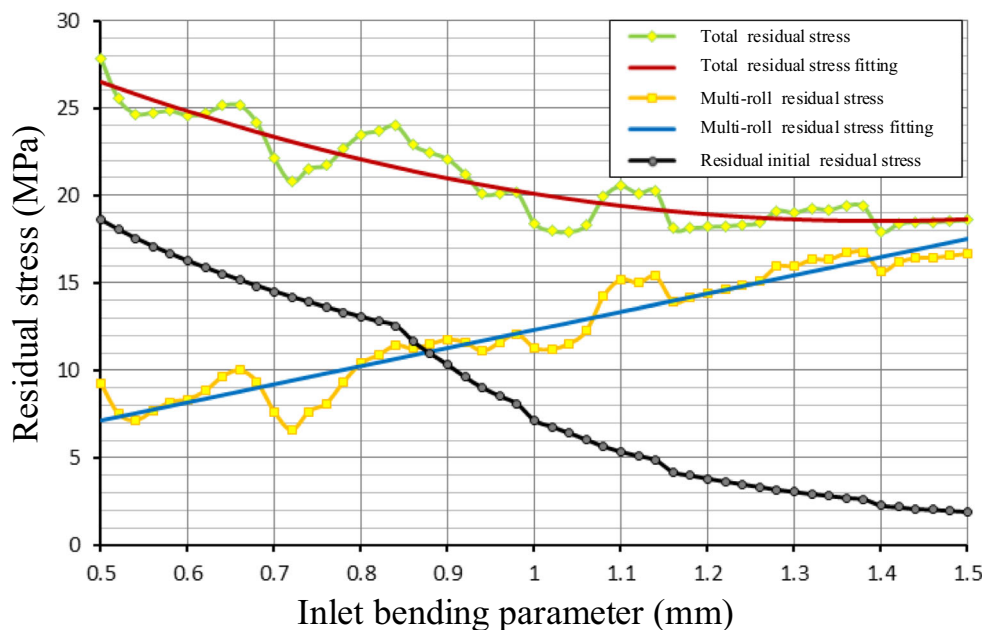

Fig. 9 Effect of the bending value on the residual wave height

Fig. 10 Residual stress changes with inlet bending parameter

parameter is 1.2 mm. The residual wave height after levelling decreases initially and subsequently increases as the maximum bending value increases because an appropriate bending value can reduce the wave defects, whereas an excessive bending value will generate new wave defects. In addition, the best levelling effect that is realised is the reduction of the wave height from 10 to 0.95 mm, which is not close to zero; hence, the roll curve needs further optimisation.

The residual stress changes with the inlet bending parameter in the levelling process as shown in Fig. 10. The total residual stress is the sum of the multi-roll residual stress and the residual initial residual stress. With the increase of the inlet

bending parameter, the plastic deformation rate increases, the multi-roll residual stress increases, and the residual initial residual stress decreases accordingly. The overall result is the reduction of the total residual stress after levelling, and the absolute average value of residual stress is reduced from 40 MPa before levelling to 18.5 MPa.

Figure 11 shows the residual curvature of a sheet with an initial curvature of -0.11 m^{-1} after the levelling of the inlet bending parameter is 0.5~1.4 mm and the outlet bending parameter is -0.3~0.3 mm. The residual curvature looks like a wave. From the top view, the wave rotates approximately clockwise around the Q point; the peak value of the wave

Fig. 11 Residual curvature changes with inlet and outlet bending parameters
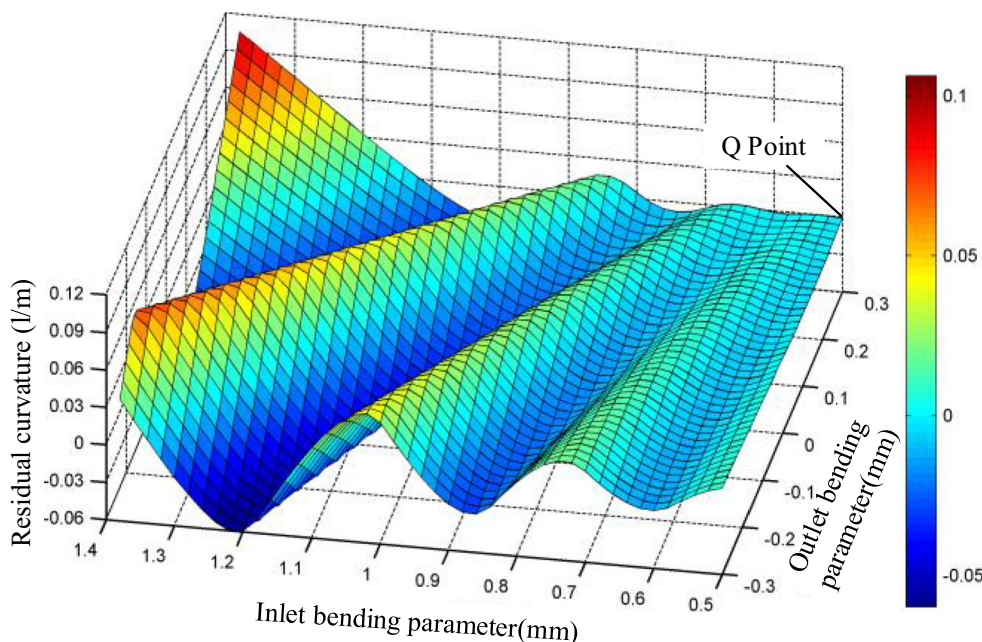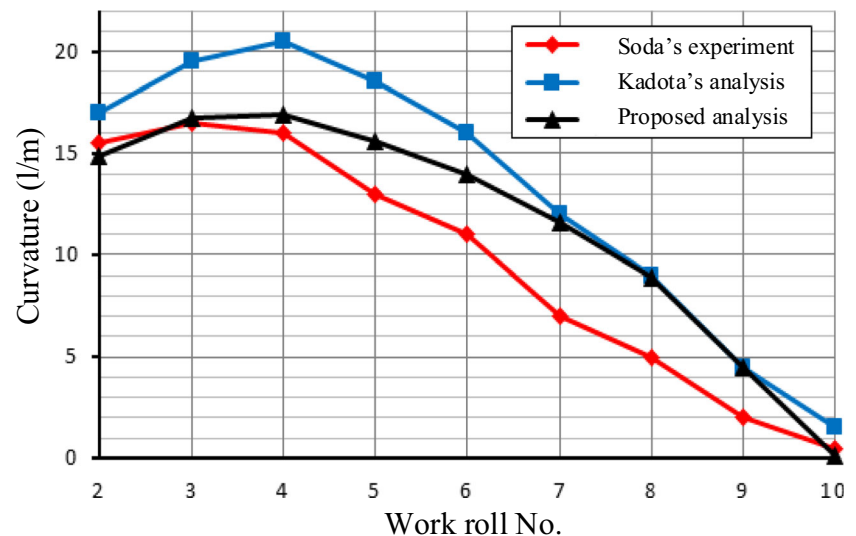
Fig. 12 Comparison of calculation results of work roll curvature

increases with the rotation. For a certain inlet bending parameter, corresponding to a plurality of outlet bending parameters, the residual curvature can be zero. Conversely, for a certain outlet bending parameter, there is also a corresponding amount of inlet bending parameters to make the residual stress zero. With the increase of the inlet and outlet bending parameters, the residual curvature shows an increasing trend, and the levelling effect deteriorates.

Soda measured the curvature distribution of the multi-roll levelling by experiments [35]; the experiment condition is as follows: the number of work rolls is 10, the diameter of work roll is 40 mm, the distance between work rolls is 42 mm, the yield stress is 180 MPa, the modulus of elasticity is 210 GPa, thickness of sheet is 0.8 mm, inlet bending parameter is 1.20 mm, and outlet bending parameter is − 0.2 mm. The comparison of proposed calculation result, Soda's experiment, and Kadota's analysis [35] is shown in Fig. 12. It can be seen that the proposed result of curvature calculation is closer to the real experimental result than Kadota's result.

7 Conclusions

Aiming at the problem that the bending characteristics of the work rolls are difficult to describe effectively in the finite element model of the multi-roll levelling, an expressing method of the convex work rolls based on the BMM is proposed. A beam element is used to express the mechanical characteristics of the work roll, and the membrane elements are used to express the contact characteristics between the work rolls and the sheet. A finite element model of multi-roll levelling based on the BMM is established, and the influence of the bending parameters on the wave levelling performance is analysed. The residual stress and curvature are discussed. The results demonstrate that selecting an appropriate bending value for

the work rolls can substantially reduce the residual waves of the levelled sheet; however, work rolls with a parabolic bending curve cannot completely eliminate the wave defects. Therefore, it is necessary to establish better bending distribution functions for wave defects in future research. In addition, the method that was studied in this paper is based on the finite element model; hence, the calculation time is long. A more efficient mathematical model should be established and combined with neural networks and other methods to realise real-time solution of multi-roll wave levelling.

References

1. Fischer FD, Rammerstorfer FG, Friedl N, Wieser W (2000) Buckling phenomena related to rolling and levelling of sheet metal. Int J Mech Sci 42(10):1887–1910. https://doi.org/10.1016/S0020-7403(99)00079-X

2. Abdelkhalek S, Montmitonnet P, Legrand N, Buessler P (2008) Manifested flatness predictions in thin strip cold rolling. Int J Mater Form 1(1):339–342. https://doi.org/10.1007/s12289-008-0064-6

3. Nakhoul R, Montmitonnet P, Abdelkhalek S (2012) Flatness defect in thin strip cold rolling and the friction impact on it. Trans N Am Manuf Res Inst 40:277–286

4. Nakhoul R, Montmitonnet P, Legrand N (2015) Manifested flatness defect prediction in cold rolling of thin strips. Int J Mater Form 8(2): 283–292. https://doi.org/10.1007/s12289-014-1166-y

5. Lopez C, Garcia DF, Usamentiaga R, Gonzalez D, Gonzalez JA (2005) Real time system for flatness inspection of steel strips. Proc Soc Photo-Opt Inst 5679:228–238. https://doi.org/10.1117/12.585902

6. Uppgård T (2008) Estimation of post-rolling effects in cold rolled aluminium strips. Licentiate thesis, Örebro University Studies in Technology Series.

7. Nakhoul R, Montmitonnet P, Potier-Ferry M (2015) Multi-scale method for modeling thin sheet buckling under residual stresses in the context of strip rolling. Int J Solids Struct 66:62–76. https://doi.org/10.1016/j.ijsolstr.2015.03.028

8. Doege E, Menz R, Huinink S (2002) Analysis of the levelling process based upon an analytic forming model. CIRP Ann-Manuf Technol 51(1):191–194. https://doi.org/10.1016/S0007-8506(07)61497-8

9. Silvestre E, Garcia D, Galdos L, de Argandona ES, Mendiguren J (2016) Roll levelling semi-analytical model for process optimization. J Phys Conf Ser 734(3):32–34. https://doi.org/10.1088/1742-6596/734/3/032034

10. Chen W-H, Liu J, Cui Z-S, Wang Y-J, Wang Y-R (2015) A 2.5-dimensional analytical model of cold leveling for plates with transverse wave defects. J Iron Steel Res Int 22(8):664–671. https://doi.org/10.1016/S1006-706x(15)30055-8

11. Grüber M, Hirt G (2017) A strategy for the controlled setting of flatness and residual stress distribution in sheet metals via roller levelling. Procedia Eng 207:1332–1337. https://doi.org/10.1016/j.proeng.2017.10.892

12. Behrens BA, El Nadi T, Krimm R (2011) Development of an analytical 3D-simulation model of the levelling process. J Mater Process Technol 211(6):1060–1068. https://doi.org/10.1016/j.jmatprotec.2011.01.007

13. Baumgart M, Steinboeck A, Kugi A, Raffin-Peyloz G, Irastorza L, Kiefer T (2012) Optimal active deflection compensation of a hot leveler. IFAC Proc Vol 45(23):30–35. https://doi.org/10.3182/20120910-3-jp-4023.00009

14. Liu Z-F, Wang Y-Q, Ou H-G, Yan X-C, Luo Y-X (2014) An analytical leveling model of curvature and residual stress simulation for H-beams. J Constr Steel Res 102:13–23. https://doi.org/10.1016/j.jcsr.2014.06.010

15. Brauneis R, Baumgart M, Steinboeck A, Kugi A, Jochum M (2017) Deflection model of a multi-actuator gap leveler. IFAC Papersonline 50(1):11295–11300. https://doi.org/10.1016/j.ifacol.2017.08.1647

16. Brauneis R, Steinboeck A, Jochum M, Kugi A (2018) A robust real-time model for plate leveling. IFAC Papersonline 51(2):61–66. https://doi.org/10.1016/j.ifacol.2018.03.011

17. Yu G, Zhai R, Zhao J, Ma R (2017) Theoretical analysis and numerical simulation on the process mechanism of two-roller straightening. Int J Adv Manuf Technol 94(9-12):4011–4021. https://doi.org/10.1007/s00170-017-1120-5

18. Yan Y, Wang H-B, Li Q, Qian B, Mpofu K (2014) Simulation and experimental verification of flexible roll forming of steel sheets. Int J Adv Manuf Technol 72(1-4):209–220. https://doi.org/10.1007/s00170-014-5667-0

19. Feng X, Montmitonnet P, Yang Q, He A, Wang X (2017) An advanced 3D mathematical model for a 6-high tandem cold rolling process. Procedia Eng 207:1379–1384. https://doi.org/10.1016/j.proeng.2017.10.900

20. Tsang K-S, Ion W, Blackwell P, English M (2017) Validation of a finite element model of the cold roll forming process on the basis of 3D geometric accuracy. Procedia Eng 207:1278–1283. https://doi.org/10.1016/j.proeng.2017.10.883

21. Laugwitz M, Seuren S, Jochum M, Hojda S, Lohmar J, Hirt G (2017) Development of levelling strategies for heavy plates via controlled FE models. Procedia Eng 207:1349–1354. https://doi.org/10.1016/j.proeng.2017.10.895

22. Woo Y-Y, Han S-W, Hwang T-W, Park J-Y, Moon Y-H (2018) Characterization of the longitudinal bow during flexible roll forming of steel sheets. J Mater Process Technol 252:782–794. https://doi.org/10.1016/j.jmatprotec.2017.10.048

23. Grüber M, Hirt G (2018) Investigation of correlation between material properties, process parameters and residual stresses in roller levelling. Procedia Manuf 15:844–851. https://doi.org/10.1016/j.promfg.2018.07.180

24. Weiss M, Rolfe B, Hodgson PD, Yang C-H (2012) Effect of residual stress on the bending of aluminium. J Mater Process Technol 212(4):877–883. https://doi.org/10.1016/j.jmatprotec.2011.11.008

25. Weiss M, Abeyrathna B, Rolfe B, Abee A, Wolfkamp H (2017) Effect of coil set on shape defects in roll forming steel strip. J Manuf Process 25:8–15. https://doi.org/10.1016/j.jmapro.2016.10.005

26. Mathieu N, Potier-Ferry M, Zahrouni H (2017) Reduction of flatness defects in thin metal sheets by a pure tension leveler. Int J Mech Sci 122:267–276. https://doi.org/10.1016/j.ijmecsci.2017.01.036

27. Traub T, Chen X, Groche P (2017) Experimental and numerical investigation of the bending zone in roll forming. Int J Mech Sci 131:956–970. https://doi.org/10.1016/j.ijmecsci.2017.07.056

28. Dratz B, Nalewajk V, Bikard J, Chastel Y (2009) Testing and modelling the behaviour of steel sheets for roll levelling applications. Int J Mater Form 2(1):519–522. https://doi.org/10.1007/s12289-009-0560-3

29. Silvestre E, de Argandona ES, Galdos L, Mendiguren J (2014) Testing and modeling of roll levelling process. Key Eng Mater 611-612:1753–1762. https://doi.org/10.4028/www.scientific.net/KEM.611-612.1753

30. Su C-J, Yang L-Y, Lou S-M, Cao G-H, Yuan F-R, Wang Q (2018) Optimized bending angle distribution function of contour plate roll forming. Int J Adv Manuf Technol 97(5–8):1787–1799. https://doi.org/10.1007/s00170-018-2053-3

31. Lee C-W, Yang D-Y, Kang D-W, Lee T-W (2014) Study on the levelling process of the current collector for the molten carbonate fuel cell based on curvature integration method. Int J Hydrog Energy 39(12):6714–6728. https://doi.org/10.1016/j.ijhydene.2014.02.043

32. Weiss M, Abeyrathna B, Pereira M (2018) Roll formability of aluminium foam sandwich panels. Int J Adv Manuf Technol 97(1-4):953–965. https://doi.org/10.1007/s00170-018-1945-6

33. Abdelkhalek S, Montmitonnet P, Legrand N, Buessler P (2011) Coupled approach for flatness prediction in cold rolling of thin strip. Int J Mech Sci 53(9):661–675. https://doi.org/10.1016/j.ijmecsci.2011.04.001

34. Abdelkhalek S, Montmitonnet P, Potier-Ferry M, Zahrouni H, Legrand N, Buessler P (2010) Strip flatness modelling including buckling phenomena during thin strip cold rolling. Ironmak Steelmak 37(4):290–297. https://doi.org/10.1179/030192310x12646889255708

35. Kadota K, Maeda R (1993) A model of analysis of curvature in levelling process-numeric study of roller levelling process. J Jpn Soc Technol Plast 34:481–486